2.B:2.G | *Nuclear Physics* **A218** (1974) 249—273;

DEUTERON STRIPPING TO THE SINGLE PARTICLE STATES OF ^{17}O†

M. D. COOPER††, W. F. HORNYAK and P. G. ROOS
University of Maryland, College Park, Maryland 20742

Received 17 July 1973
(Revised 10 October 1973)

Abstract: Angular distributions for deuteron-^{16}O elastic scattering and the $^{16}O(d, p)^{17}O$ reaction leading to levels with $E_x = 0.0$, 0.87, and 5.08 MeV have been measured at energies of 25.4, 36.0 and 63.2 MeV. The elastic deuteron data have been fit with a standard spin one optical model potential to obtain parameters for use in a DWBA analysis of the (d, p) data. The potential found in the search is shown to be consistent with other data taken in the range from 25 to 82 MeV. In addition to this deuteron optical potential, an adiabatic deuteron potential, which includes the effects of deuteron breakup, was used in the DWBA analysis. The neutron form factor was selected independent of the width of any state. The mean square radius, a single particle property, is used to find the well parameters and it determines the width of the single particle state. The spectroscopic factors obtained for the ground and first excited states are between 0.8 and 1.0 and are consistent with a large single particle parentage for these states and lower energy data. The width extracted from the DWBA analysis of the 5.08 MeV unbound state was 20% less than that obtained from elastic neutron scattering to the same state, possibly pointing up some difficulties with DWBA procedures commonly used. The adiabatic deuteron potential yields spectroscopic factors that are energy independent to 20% and gives satisfactory calculated angular distribution shapes for angles less than 40°. The conventional deuteron potential gives less satisfactory calculated shapes with the consequent introduction of some ambiguity in the derived spectroscopic factors.

E | NUCLEAR REACTION $^{16}O(d, p)$ and $^{16}O(d, d)$, $E = 25.4$, 36.0, 63.2 MeV; measured $\sigma(E; E_p, \theta)$ and $\sigma(E; E_d, \theta)$. ^{17}O deduced levels. Enriched target.

1. Introduction

Elastic neutron scattering from ^{16}O has been studied extensively [1]), and, in particular, the width of 5.08 MeV ($\frac{5}{2}^+$) state of ^{17}O has been determined accurately. States of essentially single particle character, of which the 5.08 MeV state is one, are expected to stand out clearly in a single particle transfer reaction such as $^{16}O(d, p)$. A comparison of the angular distribution from the reaction $^{16}O(d, p)^{17}O$ (5.08) to an angular distribution calculated using the distorted wave Born approximation (DWBA) should yield a width for this state [2]). The quality of the agreement between the DWBA width and the measured neutron width is a good test of the DWBA. The fact that the 5.08 MeV state is unbound, which makes the comparison possible, is not expected to affect the applicability of the results of this test to bound states. The results of ref. [2]) appear to put stripping to unbound states on an equal theoretical

† Work supported in part by the US Atomic Energy Commission.
†† NSF Predoctoral Fellow. Presently at the University of Washington, Seattle, Washington.

base with that of bound states if the measured cross section is taken as all the contributions from the resonance.

There are a number of reasons for selecting the ^{16}O reaction for this comparison. Foremost is the fact that the 5.08 MeV state of ^{17}O is one of the few predominantly single particle states which is sufficiently well separated from other nearby states to make the experiment possible at higher incident energies, where the DWBA is considered an adequate description of the reaction mechanism. Secondly is the fact that there is only one energetically available particle channel through which the 5.08 MeV state can decay, and that removes the complexity of not having the neutron width equal to the total width. Thirdly, the nature of ^{16}O as a nearly closed shell increases the chances that an optical model wave function will accurately describe the nature of the single particle states of ^{17}O. Lastly, the ^{17}O ground state ($\frac{5}{2}^+$) is a bound state with the same transferred orbital angular momentum as the 5.08 MeV state, and it provides a good comparison to the unbound state.

The spectroscopic factors and level widths derived from a DWBA analysis are supposed to be energy independent, and their deviation from a constant is also a test of the DWBA. By taking angular distributions at 25.4, 36.0 and 63.2 MeV, any energy dependence of the spectroscopic factor or level width can be measured.

Johnson and Soper [3]) proposed that the effects of deuteron breakup must be included in the deuteron optical potential in order to obtain a proper DWBA calculation. A number of recent successes which use their theory have been reported [4–6]) which cover (p, d) and (d, p) reactions on other nuclei. With this experiment, it is possible to test both the improvements in shape and the energy dependence of the spectroscopic factors resulting from the use of their prescription.

2. Experimental

Deuteron beams of 25.4, 36.0 and 63.2 MeV were obtained from the University of Maryland Cyclotron, and were energy analyzed to 0.1 %. The incident beam was focused on a gas target cell at the center of a 1.5 m diameter scattering chamber. The gas target system consisted of two gas cells with 0.005 mm Havar foil windows. During each run one cell was filled to approximately 1 atm of pressure with ^{16}O gas and the other evacuated in order to measure background. No high energy background was observed from the evacuated cell, and the lower energy background from stray beam scattering off beam line slits was judged inconsequential in the region of interest. The ^{16}O gas temperature and pressure were monitored continuously during the experiment with an accuracy better than 0.2 °C and 0.1 mm Hg respectively. No heating effects due to the energy loss of the beam in the target cell were observed. After considerable time, elastic scattering from nitrogen was observed with an intensity $\approx \frac{1}{500}$ of that from ^{16}O indicating slight, but negligible, contaminations of the target gas.

The gas target defining slits consisted of a pair of 5 mm Hevimet slits separated

by 38 cm which were precision aligned with a telescope. The angular acceptance of this slit system ranged over several values from 0.55° to 1.22°.

The scattered particles were detected with solid state detector ΔE-E telescopes. For the 25.4 and 36.0 MeV data a silicon surface barrier ΔE detector was used (500 μm at 25.4 MeV and 1000 μm at 36 MeV) in conjunction with a 4 mm Si(Li) E-detector turned at 60° to produce an effective thickness of 8 mm. This system is capable of stopping 42 MeV protons. The detector system with the gas cell slits produced an energy resolution of $\approx$ 100 keV during data accumulation.

At 63.2 MeV a Ge(Li) detector was used as the E-detector. The Ge(Li) detector was placed inside of a specially modified dewar which is mounted inside of the scattering chamber and had a holding time of 3½ days. Using side entry this detector was capable of stopping $\approx$ 100 MeV protons. With this system energy resolutions from 60 to 120 keV have been obtained for 65 MeV protons. Unfortunately, preceding the 63 MeV experiment, the detector was subjected to intense neutron bombardment which seriously radiation-damaged the detector. As a result a resolution of only 400 keV was obtained during the experiment. Thus the only data extracted at 63 MeV was the elastic scattering and the ^{16}O(d, p)^{17}O ground state transition.

Data acquisition and pulse shaping were centered around the IBM 360/44 on-line computer. Coincident ΔE and E signals were sent to 8192 channel ADC units interfaced with the computer. Using the program GELIAN [7]), the particle identification and energy addition were performed by the computer. The energy spectra of protons, deuterons and tritons were then stored in three separate analyzers.

Using a $(CH)_n$ target the scattering chamber zero angle and the beam energy were measured using differential kinematics. The zero angle was measured to better than 0.1°, and the energies were measured to be 25.4$\pm$0.2 MeV, 36.0$\pm$0.5 MeV, and 63.2$\pm$0.5 MeV. Further experimental details can be found in ref. [8]).

3. Data reduction

3.1. PEAK FITTING

With the exception of the 5 MeV states in ^{17}O, the levels considered in this experiment are well separated. A typical proton spectrum is shown in fig. 1. The peak areas for the resolved levels were obtained by summing the counts in the peak minus a linear background. This procedure leads to a uniform treatment of all of the resolved peaks, so that the relative errors are predominantly due to counting statistics. However, it is difficult to avoid approximately a 3 % error in absolute cross section. This is particularly true for the 63 MeV data which suffered from poor resolution and pile up.

The analysis of the 5.08 MeV ($\frac{3}{2}^+$) state in ^{17}O is more difficult due to the presence of two nearby states (fig. 1). The best detector resolution obtained was 100 keV, which combined with a 90 keV intrinsic width for this state, yielded a resolution insufficient to resolve the three states. Hence, an unfolding technique was used.

Vincent and Fortune [2]) point out that the "normal" procedure of subtracting a linear background for these unbound states can lead to erroneous results since a significant number of counts in the tail of the Breit-Wigner line shape can be lost. Therefore the procedure was to fit each of the three unresolved peaks (5.08, 5.22 and 5.38 MeV) with the numerical convolution of a Breit-Wigner line shape of unit area

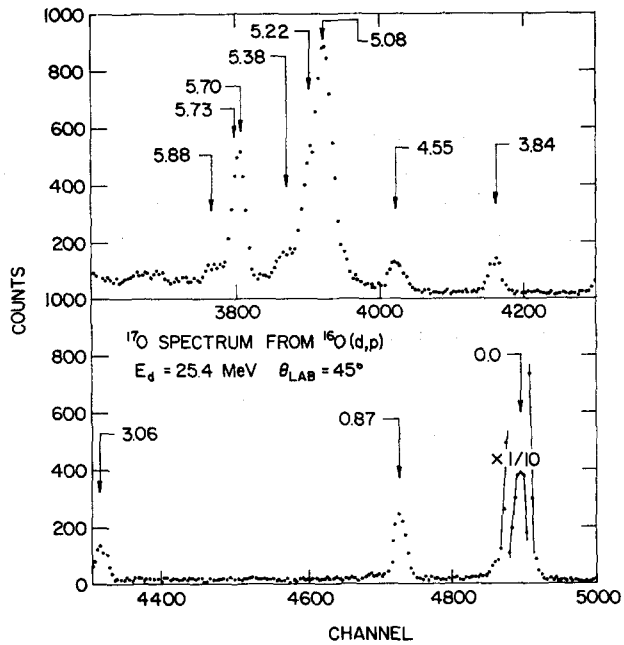

Fig. 1. The ^{16}O(d, p)^{17}O spectrum at 25.4 MeV. Every four channels have been summed. The locations of the first eleven states in ^{17}O are indicated.

and the experimental zero width shape taken from the ^{17}O ground state transition; i.e., the shape for each state k of finite width was taken to be

$$S_k(i) = \sum_{j=1}^{N} \frac{f(j)\frac{1}{2}\Gamma_k}{(i-j)^2+\frac{1}{4}\Gamma_k^2}, \tag{3.1}$$

where i is the channel number for the peak shape, j is the channel number for a shape of zero width $f(j)$ (obtained from the ground state transition), and Γ_k is the intrinsic width of the state [9]). The zero width shape $f(j)$ is normalized to unity area so that,

$$\sum_{j=1}^{N} f(j) = 1. \tag{3.2}$$

This method has the desirable feature that the tails of the Breit-Wigner line shape are automatically included, and the peak area is obtained from the normalization of the shape to the experimental spectrum. Thus, in principle, the correct peak area is obtained independent of the region in which the fitting is done.

The actual fitting procedure consisted of the following: First, the positions of the three peaks were obtained from kinematics and the location of other resolved levels. Second, a linear background was fit to the data on either side of the region of interest and subtracted. And finally, a least squares fit of the quantity

$$\text{Fit}\,(i) = \sum_{k=1}^{3} A_k S_k(i) \tag{3.3}$$

was made in which

$$\chi^2 = \sum_{i=1}^{M} W_i\{\text{Data}\,(i) - \text{Fit}\,(i)\}^2 \tag{3.4}$$

was minimized, where the W_i are the weights. Although the Breit-Wigner line shapes have been included, it is still possible to introduce an error in the peak area by the improper choice of the background. To reduce this contribution we have used equal weights for each point in the least squares fit. This procedure reduces the effects of the tails on the fitting.

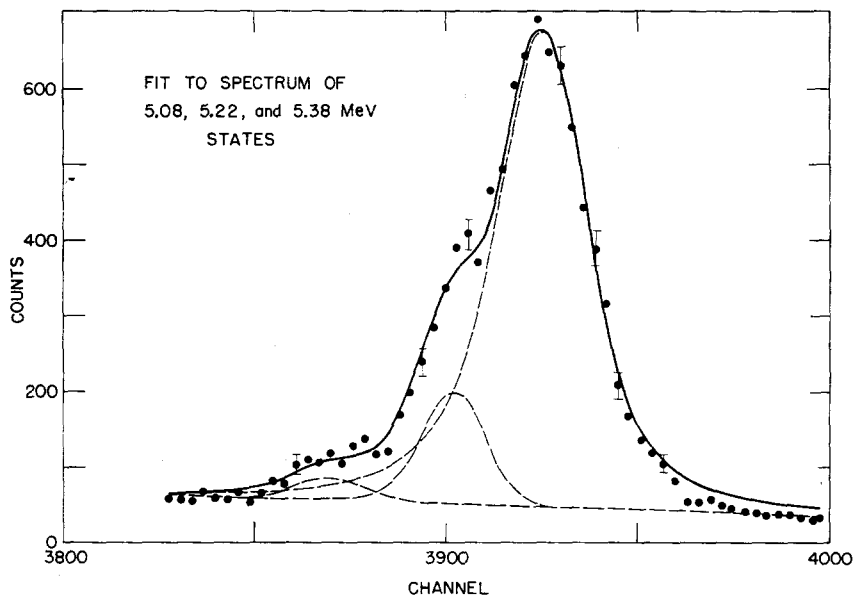

Fig. 2. A typical fit (solid line) to the three peaks present in the 5 MeV excitation energy region. Also shown are the individual contributions of each state with background added (dashed lines).

A typical fit to the experimental data is shown in fig. 2. One sees that the fit somewhat overshoots the data in the region of the tail, reflecting a possible imperfect background choice. An investigation of various background choices indicates that the background subtraction can lead to additional 3 % error beyond the normal statistical error given by the error in the A_k which are obtained through the normal least square procedure.

3.2. ABSOLUTE CROSS SECTIONS

The data were converted to absolute cross sections using the procedure of Silverstein [10]) for the gas target geometry. In addition the (d, p) data were corrected for nuclear reactions of the protons in the detector using the tables of Measday and Richard-Serre [11]). These corrections were approximately 1 %, 2 %, and 5 % for the 25, 35, and 63 MeV data. Corresponding corrections to the deuteron elastic scattering data effect the (d, p) derived quantities such as the spectroscopic factors only to second order. A crude estimate indicates that reaction corrections for deuterons should be roughly the same as for protons of the same energy, however, due to the unavailability of tabulated data these small corrections to the deuteron scattering data were not made. Their neglect should not significantly affect the quoted results.

The elastic scattering and (d, p) angular distributions at the three energies are presented in sect. 5. At forward angles the relative errors are typically 3 % and therefore smaller than the size of the plotted points. In addition an overall absolute error of 5 % is assigned based on the Faraday cup calibration, the slit measurements, etc.

4. Theory

The experimental data have been compared to theoretical calculations performed in the distorted wave Born approximation (DWBA). The DWBA for single nucleon transfer has been discussed in detail in the literature, and we present only a brief discussion here, with particular emphasis on the differences between nucleon transfer to bound and unbound states. In particular we consider the stripping reaction A(d, p)B in which B represents either a bound state in the final nucleus, or an unbound state which decays by neutron emission back to the target nucleus A.

Assuming a zero range n-p interaction the DWBA transition amplitude can be expressed as

$$T_{\mathrm{d,p}} \propto \lim_{\alpha \to 0^+} D_0 \int \mathrm{d}^3 r_{\mathrm{n}}\, \chi_{\mathrm{n}}^{(-)*}(\boldsymbol{r}_{\mathrm{n}}) \chi_{\mathrm{p}}^{(-)*} \left(\frac{M_{\mathrm{A}}}{M_{\mathrm{B}}} \boldsymbol{r}_{\mathrm{n}}\right) \chi_{\mathrm{d}}^{(+)}(\boldsymbol{r}_{\mathrm{n}}) \mathrm{e}^{-\alpha r_{\mathrm{n}}}. \tag{4.1}$$

In this expression D_0 is the usual factor introduced by invoking the zero range approximation, and $\chi_{\mathrm{d}}^{(+)}$ and $\chi_{\mathrm{p}}^{(-)}$ represent the distorted waves of the incoming deuteron and outgoing proton, respectively. The function $\chi_{\mathrm{n}}^{(-)}$ represents the wave function in the transferred neutron (either bound or unbound) and will be discussed in detail below. The factor $\mathrm{e}^{-\alpha r_n}$ has been added to the normal DWBA amplitude to insure convergence of the integrals for the case of unbound final states. The necessity of this convergence factor has been discussed in detail by Huby and Mines [12]).

The evaluation of this transition amplitude proceeds via a partial wave expansion of each of the distorted wave functions, assuming that the neutron is stripped into a state of pure angular momentum (l, j). (We are assuming that the angular distribution extracted for the unbound state, after background subtraction, contains only con-

tributions from a unique partial (l, j) wave.) A complete discussion of the techniques involved in the calculation of the integral in eq. (4.1) for unbound states has been given by Vincent and Fortune [2]).

Now let us consider the neutron wave function $\chi_n^{(-)}$ of eq. (4.1) for the cases of stripping to bound and unbound states. For stripping to bound states $\chi_n^{(-)}$ represents the overlap integral between the final state of the residual nucleus, and the ground state of the target nucleus. Pinkston and Satchler [13]) have shown that $\chi_n^{(-)}$ is properly the solution of a set of coupled equations, and that asymptotically it must behave as an exponentially decaying function in the separation energy. The standard technique is to replace this overlap integral by a single particle wave function calculated in a Woods-Saxon well and bound by the separation energy; i.e., we set $\chi_n^{(-)} = S^{\frac{1}{2}} U_n(r)$ where $U_n(r)$ is the single particle wave function normalized to unity and S is the spectroscopic factor. The value of S is obtained from the normalization of the DWBA cross section to the experimental data. Although the asymptotic behavior of $U_n(r)$ is in fact correct, one may be misrepresenting the interior. Even for strongly absorbed particles, such that the contributions of the nuclear interior to the DWBA integral are negligible, any error in the interior wave function will nonetheless reflect itself in the surface through the requirement of overall unit normalization. This in turn leads to an error in the extraction of S. Calculations such as those of Philpott *et al.* [14]) indicate that such errors are quite small for states which contain a large fraction of the single particle strength. However, clearly an inherent difficulty exists in general for the stripping to bound states interpreted by means of the usual DWBA techniques.

For stripping to unbound states the neutron wave function $\chi_n^{(-)}$ is a continuum wave function normalized to unit flux at infinity. As in the case of the bound state this continuum wave function is normally calculated using a Woods-Saxon potential, and again may be in error in the nuclear interior. However, the absolute normalization in the surface region and beyond is largely determined by the above requirement of unit flux at infinity. The basic difference between the wave functions used for the analysis of bound and unbound states lies in the fact that the normalization of the tail of the wave function is specified for the unbound case. Therefore, for reactions which are primarily sensitive to the tail of the neutron wave function (strongly absorbed particles), we would expect the DWBA treatment of the unbound state to be more correct – at least from the standpoint of the neutron wave function.

For our particular studies we have investigated the sensitivity of the DWBA cross section to the nuclear interior by two methods. First, we carried out DWBA calculations for neutron wave functions calculated with different Woods-Saxon wells. These wave functions are displayed in fig. 3. For the unbound $d_{\frac{3}{2}}$ state, although the difference in the wave functions in the nuclear interior is quite significant, the DWBA cross sections for 25.4 MeV incident energy differed by less than 1 % out to 100°. This result clearly verifies that the reaction is dominated by the surface region in which the normalization of the continuum neutron wave function is determined. For

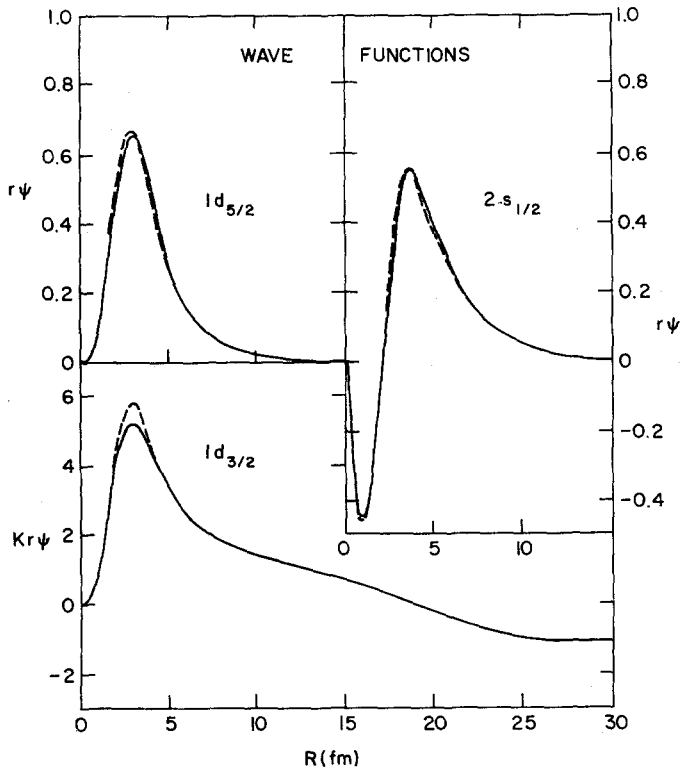

Fig. 3. Neutron wave functions used in the DWBA calculations. The two sets of curves were obtained using potential wells with different mean square radii (MSR). The solid curve has MSR = 10.76 fm^2 and the dashed curve MSR = 9.43 fm^2.

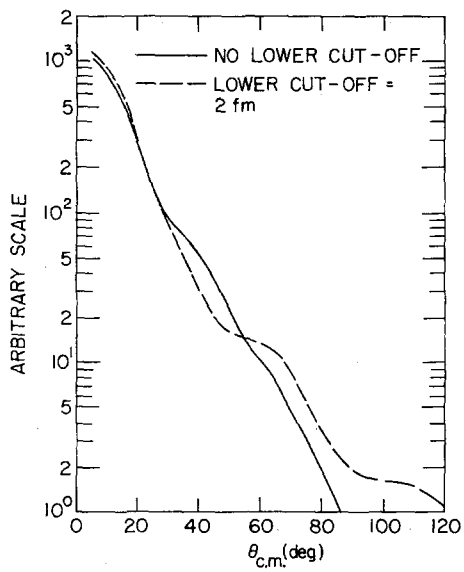

Fig. 4. DWBA angular distributions for stripping to the 5.08 MeV state ($\frac{3}{2}^+$) of ^{17}O at 63.2 MeV. The dashed curve shows the effect of a lower radial cutoff in the DWBA integral.

the bound states, the DWBA calculations with the different wave functions produce essentially the same shape for the angular distribution, but approximately a 10 % difference in magnitude. This difference in magnitude is very nearly equal to the square of the ratio of the tails of the single particle wave functions. Again this calculation shows that the DWBA cross section is primarily surface dominated, and

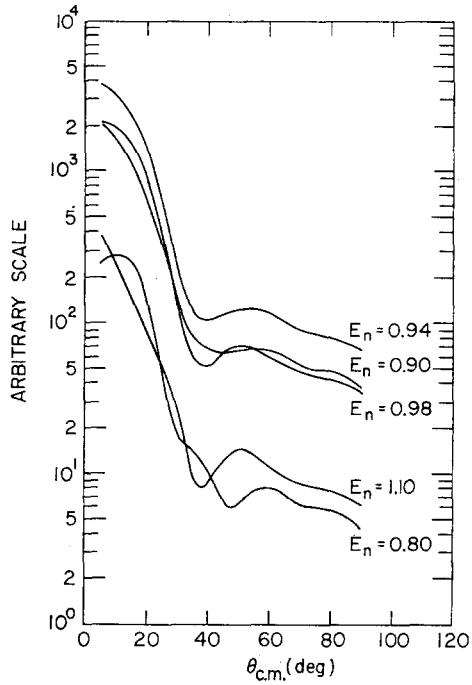

Fig. 5. DWBA angular distributions for stripping to the 5.08 MeV state ($\frac{3}{2}^+$) of ^{17}O at 25.4 MeV for various neutron separation energies.

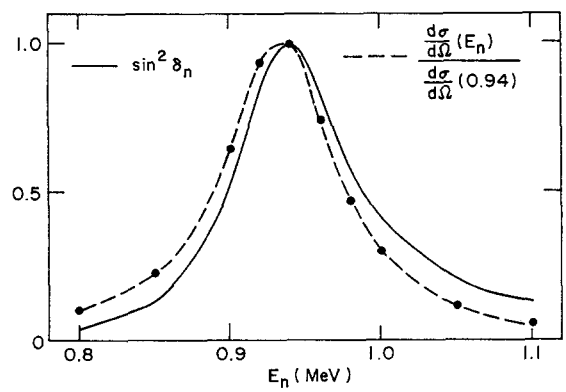

Fig. 6. Comparison of the energy dependence of the DWBA cross section as a function of the neutron separation energy to a $\sin^2 \delta_n$ dependence. The solid curve is $\sin^2 \delta_n$ and the dashed curve through the calculations was obtained for $\theta_p = 15°$ and $E_d = 25.4$ MeV.

clearly demonstrates the effect of the requirement of unit normalization of the total bound state wave function.

As a second test, we carried out calculations employing a lower radial cutoff in the DWBA integral. These calculations showed that at forward angles the calculations are quite insensitive to the nuclear interior. One such calculation is displayed in fig. 4 for 63 MeV incident energy, which corresponds to the most penetrating reaction. Even for this case the region from 5° to 30° is quite insensitive to a cutoff radius of 2 fm. As one might expect, the theoretical cross section for the lower energy data is dominated by the surface region. Thus, due to this surface dominance and the fact that the normalization of the unbound wave function is known at large radii, we expect that stripping to unbound states should be a good test of the DWBA theory for stripping reactions.

Since the unbound state (or resonance) has a finite width, care must be taken to integrate the DWBA cross section over the proper range of positive neutron energies. An estimate of the dependence of the DWBA on neutron separation energy can be made. The neutron wave function consists of a plane wave plus a scattered wave function. The largest term in eq. (4.1) is the Born term with plane waves for the incoming deuteron and outgoing proton. Because of energy conservation this term has contributions only from the scattered part of the neutron wave function; all other terms have the full wave function contributing. In the exterior region, the energy dependence of the scattered wave function is just $\sin \delta_n$, where δ_n is the neutron phase shift. Therefore, the energy dependence of the DWBA should be roughly $\sin^2 \delta_n$. The presence of the plane wave parts of the neutron wave function may modify this energy dependence and also the normalization of the calculations. Tests of the effect of the plane wave part of the neutron wave function on the normalization indicated no effect forward of 100°.

DWBA calculations of the ^{16}O(d, p)^{17}O (5.08 MeV state) reaction at 25.4 MeV have been made for ten neutron separation energies in the vicinity of neutron resonance at 0.939 MeV. The neutron continuum wave function was calculated with the Woods-Saxon well which produces a resonant state at 0.939 MeV with a width of 0.091 MeV. The angular distributions are shown in fig. 5. As expected from strong absorption considerations the distributions are remarkably similar in shape, although not exactly the same. In fig. 6 plots of $\sin^2 \delta_n$ and $[d\sigma/d\Omega(E_n)]/[d\sigma/d\Omega(0.94)]$ evaluated at 15° are shown. The shapes of the curves match reasonably well except for a slight energy shift. Similar behavior is obtained out to approximately 40°.

To sum up the contributions for all the neutron energies contributing to the apparent resonant state in the proton spectrum, an integral over the neutron energies is performed. Vincent and Fortune [2]) have shown that the cross section from the entire resonant stripping process is

$$\frac{d\sigma}{d\Omega} = \frac{2\mu_n}{\pi\hbar^2} \int_{-\infty}^{\infty} \frac{dE_n}{k_n} \frac{d\sigma^F}{d\Omega}, \tag{4.2}$$

where μ_n, k_n, and E_n are the reduced mass, momentum and energy of the neutron, and where $d\sigma^F/d\Omega$ is the cross section derived from eq. (4.1) for energy E_n with $\chi_n^{(-)}$ properly normalized. As an expedient in the evaluation of eq. (4.2), Vincent and Fortune parameterize the integrand by a Breit-Wigner shape and obtain

$$\frac{d\sigma}{d\Omega} = \frac{\Gamma\mu_n}{\hbar^2 k_n(E_R)} \frac{d\sigma^F}{d\Omega}(E_R), \tag{4.3}$$

where Γ is the width of the Breit-Wigner shape (independent of Ω) and E_R is the energy of maximum cross section. Furthermore, based on arguments about the energy dependence similar to those above, they have postulated that Γ is the same width as that obtained from neutron elastic scattering studies.

A test of this postulate has been performed to verify the accuracy of eq. (4.3) using the DWBA results presented in fig. 5. Assuming the energy dependence of eq. (4.2) is the Breit-Wigner shape of width $\Gamma = 0.091$ MeV, the integral should be

$$f \frac{\pi\Gamma}{2} \left(\frac{1}{K_n} \frac{d\sigma^F}{d\Omega}\right)_{peak}, \tag{4.4}$$

where f is a factor which depends on the energy range of integration. If that range is $[-\infty, \infty]$, then $f = 1$. For our choice of energies, $E_n = 0.8$–1.1 MeV, $f = 0.84$ and is less than one because the tails of the shape are not included in the range of numerical integration. The result of the numerical integral agrees with eq. (4.4) to better than 3 % at all angles from 5° to 90°. Hence, all of the assumptions of eq. (4.3) seem to be verified. This answer does not seem so surprising in light of fig. 6 where the area under the solid and dashed curves is about the same even though the two curves appear to have different centroids.

If the calculations for the value of $(d\sigma^F/d\Omega)_{peak}$ are believed reliable, then eq. (4.3) can be used to solve for the width Γ. Since $(d\sigma^F/d\Omega)_{peak}$ does not depend greatly on the properties of the well used to generate the neutron wave functions and only on the energy of the state, then Γ can be expected to be relatively independent of the neutron well parameters, including the width of the resonance in the well. If by some other means a single particle width $\Gamma_{s.p.}$ is known, then one can define a spectroscopic factor $S \approx \Gamma/\Gamma'_{s.p.}$, where $\Gamma'_{s.p.}$ is $\Gamma_{s.p.}$ adjusted for the energy dependence of the penetration factor to be correct for the energy of the observed resonance. If one now wishes to use the above formalism to extract Γ from a stripping reaction, one must test the accuracy of $(d\sigma^F/d\Omega)_{peak}$; i.e., the accuracy of the DWBA formalism. Such tests can be made in cases in which the width of the state has been measured by elastic scattering. If Γ obtained from the stripping through the use of eq. (4.3) does not agree with Γ found from elastic scattering, then only the value of $(d\sigma^F/d\Omega)_{peak}$ can be at fault. Put another way, if the width for elastic scattering is used to constrain the well generating the neutron wave functions, then $d\sigma/d\Omega$ calculated using eq. (4.3) must agree with the data if the DWBA is correct. In this paper, an attempt is made to test the DWBA with the $^{16}O(d, p)^{17}O$ (5.08 MeV state) reaction.

As a final point regarding the stripping to the unbound states, the "pseudo-bound" approximation, popularized by the work of Huby [15]) and Youngblood *et al.* [16]) should be mentioned. What they propose is to combine eqs. (4.3) and $S \approx \Gamma/\Gamma'_{\text{s.p.}}$ through the use of a special normalization of the scattering wave function. The result is a directly achieved spectroscopic factor which in the above formalism could be obtained from using eq. (4.3). There is no essential saving in the calculation, and there is a considerable loss in that the DWBA is never checked except through the more obscure comparison of reduced widths.

5. DWBA analysis

The use of the DWBA, discussed in the previous section, requires optical model potentials for the neutron (real potential), proton, and deuteron. In this section we present not only the calculations but also a discussion of the choice of the potentials. The optical potential is parameterized in the standard manner as

$$V_{\text{opt}} = -Vf(x) - iWf(x') - iW_{\text{s}}g(x'_{\text{s}}) - \left(\frac{\hbar}{m_\pi c}\right)^2 V_{\text{s.o.}}(\boldsymbol{L}\cdot\boldsymbol{\sigma})\left(\frac{1}{r}\frac{\text{d}}{\text{d}r}\right) f(x_{\text{s.o.}}) + V_{\text{C}}, \quad (5.1)$$

where $f(x_i) = [1+\exp(x_i)]^{-1}$, $x_i = (r - r_{0i}A^{\frac{1}{3}})/a_i$, and V_{C} is the Coulomb potential of a uniformly charged sphere of radius $r_{\text{C}}A^{\frac{1}{3}}$. Two choices for the surface imaginary potential are used; a derivative Woods-Saxon

$$g_{\text{WS}}(x'_{\text{s}}) = 4\frac{\text{d}}{\text{d}x_{\text{s}}} f(x'_{\text{s}}) \quad \text{with} \quad x'_{\text{s}} = \frac{r - r'_{0\text{s}}A^{\frac{1}{3}}}{a'_{\text{s}}}, \quad (5.2)$$

and a Gaussian surface imaginary

$$g_{\text{G}}(x'_{\text{s}}) = \exp(-x'^2_{\text{s}}) \quad \text{with} \quad x'_{\text{s}} = \frac{0.69(r - r'_{0\text{s}}A^{\frac{1}{3}})}{a'_{\text{s}}}. \quad (5.3)$$

The selection of a Gaussian surface imaginary potential is prompted by the extensive fitting to ^{16}O-proton elastic scattering data from 23–53 MeV by Van Oers and Cameron [17]). In the case of the proton and deuteron potentials particular emphasis has been placed on obtaining a consistent set of potentials as a function of energy. For the neutron the potential was chosen to fit available information on the ^{16}O+n system.

5.1. DEUTERON POTENTIALS

Two types of ^{16}O-deuteron potentials are employed in the present analysis; those which fit elastic deuteron scattering data and those constructed according to the adiabatic model of Johnson and Soper [3]).

The conventional deuteron potentials were obtained from optical model fits to the elastic scattering data obtained in this experiment. These fits were carried out using the computer program HUNTER [18]). Two restrictions are placed on the parameters

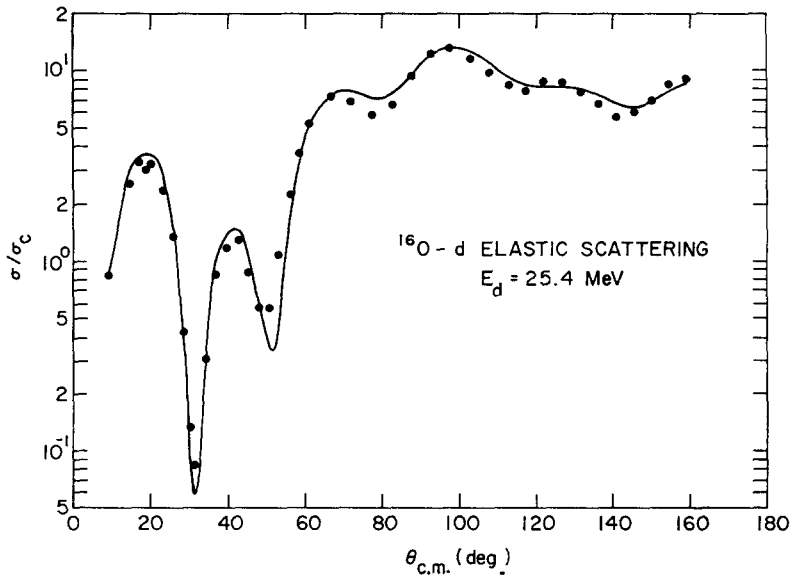

Fig. 7. Optical model fit to the deuteron elastic scattering data at 25.4 MeV.

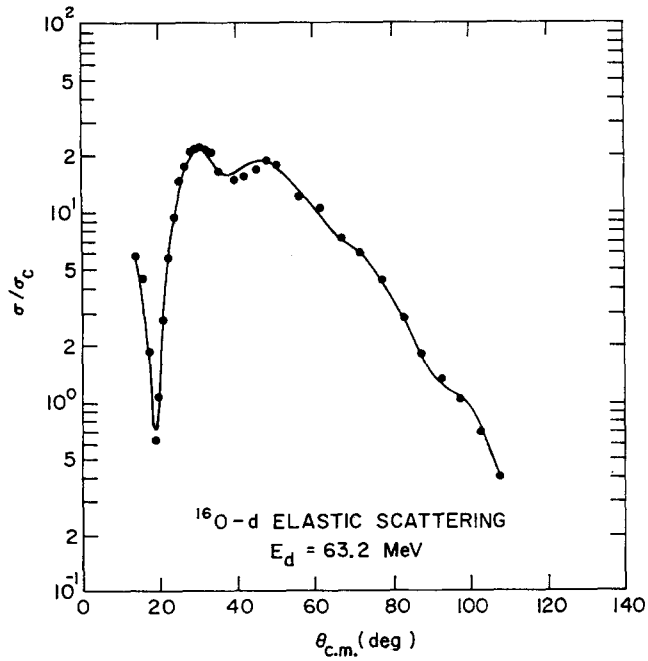

Fig. 8. Optical model fit to the deuteron elastic scattering data at 63.2 MeV.

to reduce the number of free variables. The first is to set the geometric parameters of the spin-orbit well equal to those of the real well as has been done in previous analyses [19-23]). The second restriction was to choose the real well radius parameter $r_0 = 1.05$ fm. It was an important premise of the optical model fitting to choose a potential which had a smoothly varying character as a function of energy. Such a comparison was only simple if the potentials had similar geometries, and $r_0 = 1.05$ fm is a rather common choice in the literature [22, 23]). Additional searches were performed releasing the restriction on r_0. Although χ^2 was found to improve slightly, the resulting DWBA calculations using these new potentials differed by less than 5 % in the first 40°, and less than 20 % at 80°.

TABLE 1

Deuteron-^{16}O optical potential parameters used in the DWBA calculations

E (MeV)	Equation [a])	V (MeV)	r_0 (fm)	a (fm)	W_D (MeV)	r'_{0s} (fm)	a'_s (fm)	$V_{s.o.}$ (MeV)	$r_{0\,s.o.}$ (fm)	$a_{s.o.}$ (fm)	r_C (fm)	χ^2/N
25.4	5.2	94.79	1.05	0.843	8.58	1.573	0.573	6.98	1.05	0.843	1.3	6.1
34.6	5.2	92.84	1.028	0.796	8.84	1.409	0.697	7.57	1.028	0.796	1.3	
63.2	5.2	83.13	1.05	0.782	8.78	1.290	0.776	4.41	1.05	0.782	1.3	1.5
25.4	5.3	106.2	1.142	0.756	22.3	1.268	0.761	6.0	1.114	0.585	1.3	
36	5.3	101.9	1.142	0.756	19.2	1.268	0.761	6.0	1.114	0.585	1.3	
63.2	5.3	92.1	1.142	0.756	13.9	1.268	0.761	6.0	1.114	0.585	1.3	

The first group is derived from fitting elastic scattering data, while the second group includes deuteron breakup via the adiabatic model. The notation is that of eqs. (5.1)-(5.3).

[a]) Specifies the equation used for the form of the surface imaginary potential.

In addition, only the surface imaginary potential was employed; i.e., $W = 0$. Several studies [22-24]) of ^{16}O-deuteron elastic scattering from 34 to 82 MeV have shown that only a surface imaginary well is required. The results of the optical model searches are shown in figs. 7 and 8. The parameters used in the DWBA calculations in the "conventional" treatment are listed in the first part of table 1. For the 36 MeV data, the 34.6 MeV parameters of ref. [22]) were used.

The parameters in table 1 show a smooth variation with energy. Furthermore, the root mean square radii of the potentials are nearly the same, and the volume integrals of the potentials exhibit a smooth energy dependence. Both quantities are consistent with previous optical model results [22-24]). Thus, a consistent set of deuteron optical potentials was used in the DWBA analysis.

The second type of deuteron potential used in the DWBA analysis is that constructed using the adiabatic model of Johnson and Soper [3]). They have shown that the contributions of deuteron breakup into a relative S-state can be included in the DWBA by constructing the deuteron optical potential from neutron and proton optical

potentials at half the deuteron energy by the following prescription:

$$V(\boldsymbol{R}) = D_0^{-1} \int \mathrm{d}\boldsymbol{r}[V_\mathrm{n}(\boldsymbol{R}+\tfrac{1}{2}\boldsymbol{r}) + V_\mathrm{p}(\boldsymbol{R}-\tfrac{1}{2}\boldsymbol{r})]V_\mathrm{np}\,\phi_\mathrm{d}(\boldsymbol{r}), \tag{5.5}$$

$$D_0 = \int \mathrm{d}\boldsymbol{r}\, V_\mathrm{np}\,\phi_\mathrm{d}(\boldsymbol{r}).$$

The quantities V, V_n, V_p, and V_np are the deuteron, neutron, and proton optical potentials and neutron-proton potential, respectively, ϕ_d is the wave function of the deuteron, $\boldsymbol{r}$ is the p-n relative coordinate, and $\boldsymbol{R}$ is the c.m. coordinate of the deuteron.

Satchler [25]) has developed approximate formulae for nuclear Woods-Saxon potentials which allow one to bypass the actual evaluation of the integral in eq. (5.5). This treatment allows one to easily obtain a Woods-Saxon deuteron potential from the proton potential (assumed to be the same as the neutron potential) at one half the deuteron energy. The same type of technique was used to treat the Gaussian surface imaginary potential of the proton optical model.

A number of applications [4–6]) of the adiabatic theory to nucleon transfer reactions have been quite successful in giving reasonable DWBA fits to data covering a wide range of masses. In the light nuclei, the need for a lower radial cut-off in the DWBA integral is removed, and the general features of the experimental angular distributions are better reproduced than for calculations using a deuteron optical potential derived from elastic scattering.

The adiabatic deuteron potential is defined once the proton potentials have been chosen. The ^{16}O-proton potentials are taken from a straight line drawn through the energy dependent fit parameters of Van Oers and Cameron [17]) for data from 23–53 MeV. Since the proton potential is required at half the deuteron energy, values at energies as low as 12.7 MeV are needed. At such low energies the optical model is in serious question; therefore, scattering data at these energies are not used, and an extrapolation of the line from 23 MeV down is used. Such a procedure leaves considerable ambiguity in the choice of the potential strengths. However, for consistency between energies it is adopted. There seems to be no theoretical guidance on a better prescription although McAllen *et al.* [4]) tried arbitrarily adjusting the potential strengths with no conclusion. The parameters used in the DWBA calculations are listed in the second half of table 1.

5.2. CHOICE OF NEUTRON WAVE FUNCTIONS

Single particle shell model wave functions for the bound and unbound states of ^{17}O for use in the DWBA calculations can be found by a technique similar to that used by Beres and MacDonald [26]). Their technique is to solve for the wave function in a real Woods-Saxon optical potential well with a spin-orbit interaction. The geometric parameters for the real and spin-orbit wells are set equal. With the radius parameter r_0 chosen, there are three other free parameters V, $V_\mathrm{s.o.}$, and a. These are

determined by searching until the well gives the binding energy for the $1d_{\frac{5}{2}}$ state (4.143 MeV), the separation of the $1d_{\frac{5}{2}}$ and $1d_{\frac{3}{2}}$ states (5.083 MeV) and the width for the $1d_{\frac{3}{2}}$ unbound state (0.091 MeV). Finally, keeping the geometry the same, the $2s_{\frac{1}{2}}$ wave function is obtained by further modifying the real well depth to give the $2s_{\frac{1}{2}}$ binding energy.

It is known that reasonably small changes of the radius parameter r_0 of the real well can produce changes of the order of 20 % in the DWBA cross section calculated using the bound state wave functions for these wells. However, with the above constraints, when r_0 is changed, not only V, but also $V_{s.o.}$ and a must be changed. Since there is less freedom in the parameters, it is of interest to see if the effects on the DWBA are as great. Four sets of solutions, including the one of Beres and MacDonald, are given in table 2. The solutions fall along the Vr_0^2 ambiguity with slight modifications to the diffuseness and spin-orbit well strength.

TABLE 2

Neutron-^{16}O optical potential parameters which fit the properties of the 0.0, 0.87, and 5.08 MeV states of ^{17}O

r_0 (fm)	V (1d states) (MeV)	V (2s state) (MeV)	a (fm)	$V_{s.o.}$ (MeV)	Vr_0^2 (MeV · fm^2)	MSR (fm^2)	Volume-integral (MeV · fm^3)
1.250	52.561	54.967	0.5234	5.332	82.13	9.434	696.75
1.281 [a])	50.117		0.5035	5.384	82.24	9.434	696.78
1.300	48.672		0.4888	5.409	82.26	9.410	695.65
1.350	45.099	49.330	0.4514	5.517	82.19	9.405	694.69

The notation is that of eq. (5.1).
[a]) See ref. [26]).

The resulting wave functions for $r_0 = 1.25$ fm are shown as dashed curves in fig. 3; the wave functions for the other values of r_0 would be nearly indistinguishable on the plot. The bound state wave functions are normalized such that

$$\int_0^\infty |\psi|^2 r^2 dr = 1, \tag{5.6}$$

and the unbound state is normalized so that

$$Kr\psi \underset{r\to\infty}{\to} \sin(Kr+\delta). \tag{5.7}$$

The two solutions for $r_0 = 1.25$ and 1.35 fm have been used to calculate the angular distributions for the $1d_{\frac{5}{2}}$ and $2s_{\frac{1}{2}}$ states. The resulting curves are nowhere different by more than 6 %, and at forward angles are the same to 3 %. Compared to other uncertainties, the ambiguity in the spectroscopic factor due to the radius parameter is negligible, and henceforth, a value of $r_0 = 1.25$ fm was used.

One obvious criticism of the above technique is using the width of the 5.08 MeV state to define the single particle well since this state may not have a purely single particle character. It can be numerically verified that knowing the width of $1d_{\frac{3}{2}}$ state in a Woods-Saxon well is equivalent to knowing the mean square radius (MSR) of that well. Table 2 shows that the MSR of all of the potentials are the same. Furthermore, Sharpey-Schafer [27]) has demonstrated for ^{53}Cr and ^{91}Zr that if the MSR of the potential is held constant and the radius and diffuseness are allowed to vary, then the resulting DWBA calculations are nearly identical. In that light, the fact that the potentials of table 2 produce nearly equivalent DWBA angular distributions is not surprising.

What these observations point up is that there are really only three unknowns to be fit with the d-wave optical potential: The two energies of levels and the MSR of the potential. There are two ways to choose the MSR of the well. The first would be to use the mean square radius obtained from doing optical model fits to elastic neutron scattering data at high energies. Unfortunately, no such data exist above 15 MeV and very few exist below 15 MeV where the presence of numerous levels adds further complications.

The second technique, which is the one adopted here, is to estimate the MSR from electron scattering experiments. Since ^{16}O has an equal number of protons and neutrons, it is reasonable to assume the proton and neutron mass distributions are the same. The charge radii of nuclei are quite accurately measured by electron scattering experiments, and the most current result [28, 29]) for ^{16}O is a MSR of 7.129 fm^2. This value must be corrected for the finite charge radius of the proton, taken as 0.64 fm^2, and the MSR of the nucleon-nucleon interaction, taken as 4.27 fm^2 from Greenlees *et al.* [30]). As pointed out by these authors, there is considerable error in the last number for the nucleon-nucleon interaction, and this error will produce at most a 10 % uncertainty in any deduced spectroscopic factors for bound states. The resulting MSR is 10.76 fm^2. Choosing r_0 to be 1.25 fm, a diffuseness parameter of 0.590 fm results. Using these values of r_0 and a and searching on V and $V_{s.o.}$ to fit the binding energy of the $1d_{\frac{3}{2}}$ state and $1d_{\frac{5}{2}}$–$1d_{\frac{3}{2}}$ separation, V is found to be 52.675 MeV and $V_{s.o.}$ is found to be 5.794 MeV. The width of the $1d_{\frac{3}{2}}$ state is then calculated to be 102.2 keV, somewhat larger than the 91 keV assumed for table 2, and is independent of the choice of r_0. Using the same geometry, V (2s state) = 54.072.

The single particle wave functions for the states of interest are the solid curves in fig. 3. It is obvious that the curves are quite similar in shape to the dashed curves, and in fact, for the purpose of illustration, the differences have been slightly exaggerated. As stated in sect. 4 the dominant region of configuration space is the surface just outside the root mean square radius of 3.28 fm. Although the $1d_{\frac{3}{2}}$ wave function appears to be the most different, DWBA calculations performed with both $1d_{\frac{3}{2}}$ curves gave identical distributions out to 100°. The $1d_{\frac{5}{2}}$ and $2s_{\frac{1}{2}}$ curves differ from their dashed curves by only 3 % in the critical region, but the DWBA curves differed by about 10 %.

Hence, it can be seen that picking the proper single particle well is particularly important in order to get accurate spectroscopic factors for bound states. To reiterate, for bound states the effects of the complexities of the interior region are manifest in the normalization of the wave function, while for unbound states the normalization is fixed and the DWBA is largely insensitive to the interior wave function.

5.3. CHOICE OF ^{17}O-PROTON POTENTIALS

Due to the lack of ^{17}O-proton elastic scattering measurements, the parameters of Van Oers and Cameron [17]) for ^{16}O-proton scattering are used, with a correction added for the seventeenth particle. The correction due to the last neutron is somewhat uncertain, but the technique is less dubious because the last particle is expected to produce only roughly $\frac{1}{17}$ of the total potential. Watson *et al.* [31]) have studied mass

TABLE 3

Proton-^{17}O optical potential parameters used in the DWBA calculations

$r_0 = 1.142$ fm	$a = 0.726$ fm	$V_{s.o.} = 6.0$ MeV
$r'_0 = r'_{0s} = 1.268$ fm	$a' = a'_s = 0.676$ fm	
$r_{0\,s.o.} = 1.114$ fm	$a_{s.o.} = 0.585$ fm	
$r_C = 1.3$ fm		

State in ^{17}O	E_{lab} (MeV)	V (MeV)	W (MeV)	W_D [a]) (MeV)
0.0	25.9	50.3		9.6
0.87	25.0	50.7		9.8
5.08	20.6	52.3		10.8
0.0	35.9	46.7	1.40	7.5
0.87	35.0	47.0	1.15	7.7
5.08	30.5	48.6		8.7
0.0	61.5	37.4	7.85	1.9
5.08	56.1	39.4	6.0	3.1

The strengths have been modified to account for the energy dependence of the wells. The notation is that of eqs. (5.1) and (5.3).

[a]) Gaussian surface imaginary potential.

effects in the 1p shell and give mass dependent equations for the potentials. Their results imply a change in the strengths of the potentials due to the last neutron of 1.4 MeV in the real potential and 0.7 MeV for the surface imaginary potential. Obviously, the use of these corrections is rather crude since they are obtained from optical potentials for different nuclei. However, since the corrections are small, any errors should not significantly affect the DWBA results.

Lerner [32]) has measured proton elastic scattering from ^{17}O at 65 MeV and has performed optical model fits to the data. His well depth was corrected to obtain values for 61.5 MeV which is appropriate to the ground state reaction for $E_d = 63.2$ MeV. The DWBA calculations made using both proton optical model parameter sets

produced nearly indistinguishable angular distributions. The ^{17}O potential parameters used are listed in table 3.

5.4. FINITE RANGE AND NON-LOCALITY

Finite range in the n-p interaction [33]) and non-locality in the deuteron and proton optical model wave functions [34]) were included by means of the local energy approximation. A range of 1.50 fm was used for the proton-neutron interaction. The

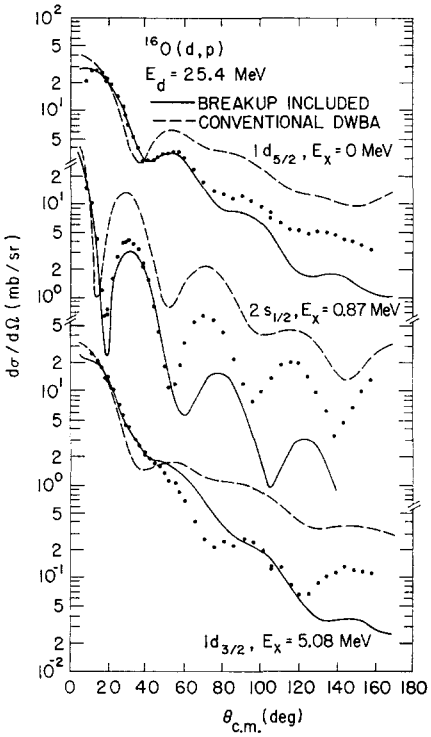

Fig. 9a. DWBA fits to the 25.4 MeV $^{16}O(d, p)^{17}O$ data. The optical model parameters are presented in tables 1–3.

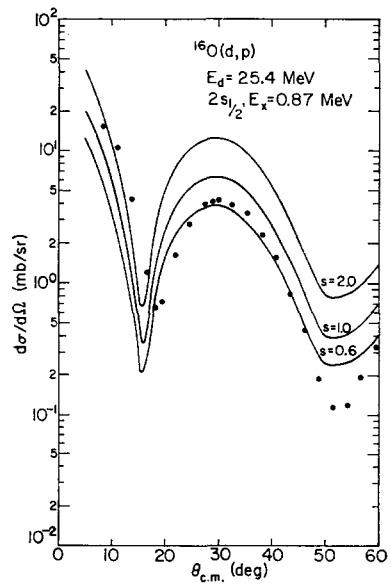

Fig. 9b. An expanded version of the $2s_{\frac{1}{2}}$ stripping results presented in fig. 9a to emphasize the difficulties in fitting to forward angle data. The curves represent DWBA calculations using the conventional potential, normalized for different spectroscopic factors.

range of non-locality was taken to be $\beta_d = 0.54$ and $\beta_p = 0.85$. The optical potential for the neutrons was assumed to be local because of the lack of a simple, correct way to include non-locality effects at low energies.

5.5. FITS

The computer code for calculating the DWBA angular distributions was originally written by Tamura [35]) and modified by Vincent and Fortune [2]) to do calculations for

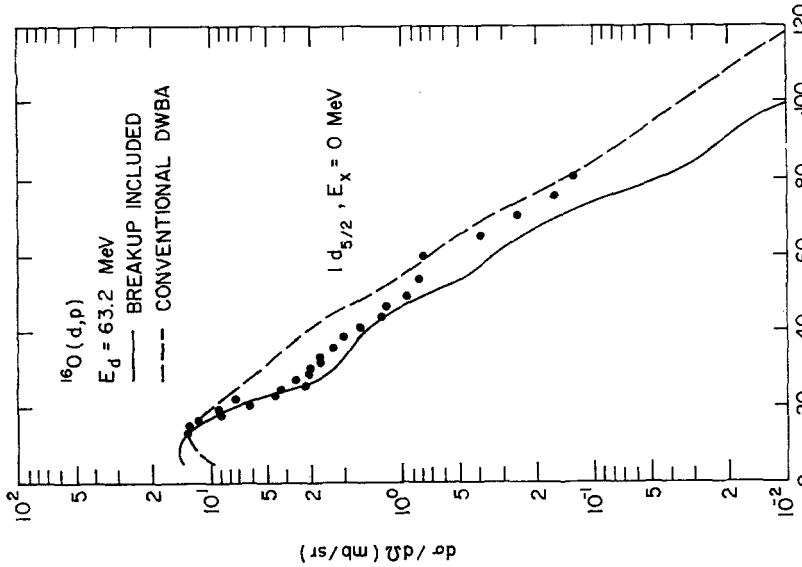

Fig. 11. DWBA fits to the 63.2 MeV ^{16}O(d, p)^{17}O data. The optical model parameters are presented in tables 1–3.

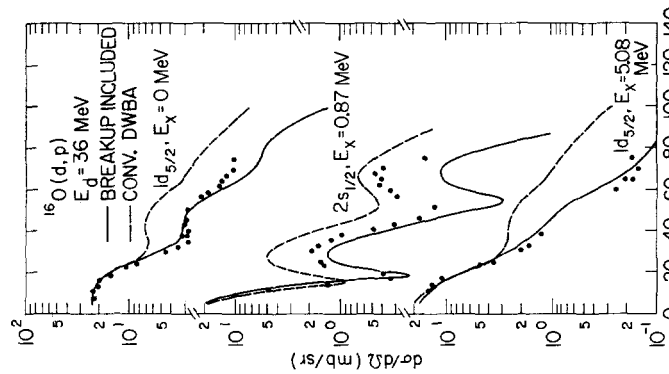

Fig. 10. DWBA fits to the 36.0 MeV ^{16}O(d, p)^{17}O data. The optical model parameters are presented in tables 1–3.

unbound states. It was modified again to run on the University of Maryland cyclotron's IBM 360/44 computer, and was shown to agree with calculations performed with the code JULIE [36]).

In what follows, calculations using a deuteron optical potential derived from elastic deuteron scattering will be referred to as "conventional" DWBA calculations and shown as broken lines in the figures. Calculations using the Johnson and Soper formalism for the deuteron potential will be referred to as "breakup included" or adiabatic DWBA calculations and shown as solid lines in the figures.

The data and fits for incident deuteron energies of 25.4, 36.0, and 63.2 MeV are shown in figs. 9–11 respectively. The most striking feature of the fits is their phasing; i.e., the relative angular location of the maxima and minimum. None of the calculations do particularly well in reproducing the large angle behavior of the experimental data. Therefore, the criteria on which they are judged is the agreement with the data at forward angles, which is where the spectroscopic information lies. The conventional DWBA curves all seem to have the location of the first minimum incorrectly predicted, and this is a serious deficiency because it makes the determination of the normalization difficult. The adiabatic calculations are a definite improvement and appear to do quite well in the first 50°. Based on the visual improvements of the fits, the adiabatic theory is judged as a superior technique for calculating deuteron stripping cross sections.

Since the spectroscopic information lies at the more forward angles, the fits must be normalized in this region. Guidance can be found in selecting the proper angular range from fig. 9. In the first 35° we find no significant departures in the DWBA cross section due to changes in the interior part of the neutron form factor. At lower energies this range might be expected to be slightly larger because the deuterons are more strongly absorbed. Hence, the calculations including breakup are normalized in the first 35° to 40°.

For the conventional DWBA the situation is more difficult because the fits are so poor even at forward angles. Since the Born approximation should be best at forward angles, the conventional calculations are normalized between 15° and 20°. Obviously with such poor fits there is a considerable uncertainty in any extracted spectroscopic factors. The problem is particularly acute for the 0.87 MeV state, and in fig. 9b there are shown several possible normalizations and the resulting spectroscopic factors.

The increased confidence in the deduced spectroscopic factors due to the improvements in the fits strongly favors the use of the deuteron optical potential which includes breakup effects.

6. Results and discussion

For bound states spectroscopic factors are obtained by comparison of DWBA calculations with experiment and for unbound states the widths can be extracted by

using eq. (4.3). Table 4 contains the spectroscopic factors and widths found for both the conventional calculations (4a) and calculations with deuteron breakup effects included (4b).

Earlier measurements [2, 37-41]) of the spectroscopic factors for the $d_{\frac{5}{2}}$, $s_{\frac{1}{2}}$, and $d_{\frac{3}{2}}$ states in ^{17}O and ^{17}F through the (d, p) and (d, n) reactions at energies E_d = 7–12 MeV generally agree with the values $S(d_{\frac{5}{2}}) = 0.8$–1.1, $S(s_{\frac{1}{2}}) = 0.9$–1.1, and $\Gamma(d_{\frac{3}{2}}) \approx 67$ keV.

TABLE 4a

Spectroscopic factors and widths for states of ^{17}O when a conventional deuteron potential is used in the DWBA calculations

E_d (MeV)	S(0.00)	S(0.87)	Γ(5.08) (keV)
25.4	0.99	1.96	73
36	1.07	1.14	74
63.2	0.96		

TABLE 4b

Spectroscopic factors and widths for states of ^{17}O when breakup is included in the deuteron potential

E_d (MeV)	S(0.00)	S(0.87)	Γ(5.08) (keV)
25.4	0.81	0.78	66
36	0.84	0.91	60
63.2	1.03		

These experiments measured spectroscopic factors relative to the ground state of ^{16}O. Brown and Green [42]) have calculated wave functions for both the ground state of ^{16}O and even parity states of ^{17}O and ^{17}F in a deformed shell model picture and have included contributions from more complicated configurations than just 1p–0h on a 0p–0h core. They give the ratio of the spectroscopic strengths in their model and, assuming that the strengths should sum to unity, the values are: $S(1d_{\frac{5}{2}}) = 1.0$, $S(2s_{\frac{1}{2}}) = 0.99$, and $S(1d_{\frac{3}{2}}) = 0.71$.

6.1. COMPARISONS OF THEORY AND EXPERIMENT

In the angular region below 40°, where the DWBA calculations might be expected to accurately apply, the breakup including potential gives a notably better fit to the data. Primarily for this reason we attach more significance to the spectroscopic factors obtained with this potential.

Prior to the proposal of the adiabatic deuteron potential, improved fits were obtained with the use of an artificial lower cutoff in the overlap integral of the

DWBA. McAllen *et al.* [4]) showed that the inclusion of deuteron breakup effects in (p, d) reactions removes the need for this lower cutoff, and our results seem to verify the conclusion for (d, p) as well.

One last point which deals with the appearance of the calculated curves concerns the downward trend to the data for the ground state (E_d = 25.4 MeV) at the most forward angles. It is doubtful that there is any experimental error in these forward angle points and further the 12 MeV data [37]) also have an even more pronounced downward trend. Neither type of fit produces this sort of behavior, and this is a serious fault of both theories because the forward angles should be required to fit best. On the other hand, the adiabatic theory is too low for the data at the most forward angles in the case of the 5.08 MeV state. This fact suggests some sort of small angle j-dependence. One explanation of such effects has been the elimination of the D-state of the deuteron in the DWBA calculations [43]).

Since the spectroscopic factor is viewed as the overlap of the product of a single particle wave function and the target ground state with the final state, the spectroscopic factor should be independent of incident deuteron energy if the DWBA analysis properly accounts for the energy dependence of the distorted waves. The experiment covers a 38 MeV range of deuteron energies, and the analysis used consistent sets of optical potentials. The spectroscopic factors measured for ^{16}O(d, p) do not show any significant deviation from this hypothesis within the usual 20 % uncertainties attributed to the effects of uncertainties in the optical potentials.

The measured neutron width for the 5.08 MeV state of ^{17}O is 94$\pm$2 keV [ref. [1])]† and that value is confirmed in a recent paper [44]). The widths in table 4 are consistently 20 % smaller than Γ_n even if a systematic correction is made to all calculations which would give the ground state S = 1. Coincidentally, this is the same discrepancy noted by Vincent and Fortune [2]) with the 12 MeV data. The value of Γ extracted from the (d, p) reaction should exactly agree with Γ_n and can only differ if $(d\sigma^F/d\Omega)_{peak}$ is improperly estimated by the DWBA.

The criticism of the DWBA is more important for the unbound state test because there is no ambiguity in the neutron wave function which significantly affects the calculation. If the 20 % discrepancy in the widths is taken seriously, there must be some part of the reaction mechanism which is not included in the DWBA which will change the relative magnitude of the ground state and 5.08 MeV state predictions. Otherwise the normal procedure of DWBA analysis so commonly used is in question.

In addition to the comparison of widths derived from stripping and elastic scattering, the stripping spectrum (e.g. fig. 1) at one angle is related to the total elastic neutron cross section as shown by Lipperheide and Mohring [45]). In particular, they

† The value of 94 keV was found with a phase shift analysis which assumed a pure resonance form for the 1 MeV anomaly. The background phase shift was assumed to be 0°, and this implies that interference effects with the background are not included in the calculation of the width. This is fortunate because no interference effects are included when extracting the areas of the stripping peaks. The interference with the background found in an R-matrix analysis only modifies the width by 0.4 keV.

predict that the stripping cross section for each transferred orbital angular momentum L will vary proportionally to the half-off-shell cross section, with the momentum transfer q in the initial state and the resonance momentum k in the final state. Young [46]) has suggested that the momentum dependence of the form factor is approximately

$$M_L(p) \propto \frac{p^L}{(p^2+\beta^2)^{\frac{1}{4}(L+2)}}, \tag{6.1}$$

where β is the range of the force (i.e., inverse nuclear radius). For two states of different L at the same energy and with the same cross section in the neutron elastic scattering channel, the relative peak heights in the stripping cross section will be

$$\frac{M_L^2(q)}{M_L^2(k)} \frac{M_{L'}^2(k)}{M_{L'}^2(q)} = \frac{q^{2L-2L'}(q^2+\beta^2)^{L'-L}}{k^{2L-2L'}(k^2+\beta^2)^{L'-L}}. \tag{6.2}$$

At $E_d = 25.4$ MeV and $\theta_p = 20°$, the momentum transfer is 0.7 fm^{-1} and the final state momentum is 0.2 fm^{-1}. In the case of ^{17}O, the 5.08 MeV state sits on a large s-wave background in the elastic scattering. From eq. (6.2) it is seen that the s-wave is very inhibited compared to the d-wave, and this accounts for the small background in fig. 2. Additionally, since the state at 5.22 MeV is not seen in elastic scattering, it is probably a high spin state; this fact is supported by the featureless angular distribution of the 5.22 MeV state. Although Lipperheide and Möhring point out that formulae like eq. (6.2) are only qualitative and intended to give guidance, some general features of the (d, p) spectra are seen to agree with their prediction. However, to avoid confusion regarding the extraction of the stripping widths because the peak height depends on the off-shell matrix elements, we note that the use of optical potential wave functions in the DWBA formalism automatically takes these off-shell effects into account.

In summary, the major results from the ^{16}O(d, p) experiment are the measurement of spectroscopic factors of around 1.0 for the bound ground and first excited states and a stripping width of around 70 keV for the unbound 5.08 MeV state. A reasonable prescription for picking the neutron optical potential well was investigated which did not depend on the width of a particular state but on a single particle property, the mean square radius. The inclusion of breakup in the deuteron optical channel made a significant improvement in the quality of the fits even though no fit is outstanding. The 70 keV stripping width was extracted from a consistent analysis of the bound and unbound states of ^{17}O and indicates possible failure of the DWBA as a tool to extract quantitative spectroscopic information because the stripping width did not equal the neutron width of 94 keV. Lastly, there was not significant energy dependence to the spectroscopic information over a 38 MeV range of incident deuteron energies.

The authors are indebted to Drs. G. M. Lerner and R. A. J. Riddle for their help during the experiment and Dr. E. F. Redish for his guidance on theoretical problems.

References

1) C. H. Johnson and J. L. Fowler, Phys. Rev. **162** (1967) 890
2) C. M. Vincent and H. T. Fortune, Phys. Rev. **C2** (1970) 782
3) R. C. Johnson and P. J. R. Soper, Phys. Rev. **C1** (1970) 976
4) G. M. McAllen, W. T. Pinkston and G. R. Satchler, Particles and Nuclei **1** (1971) 412
5) J. D. Harvey and R. C. Johnson, Phys. Rev. **C3** (1971) 636
6) B. M. Preedom, Phys. Rev. **C5** (1972) 587
7) N. R. Yoder, University of Maryland Technical Report 73–042
8) M. Cooper, Ph.D. thesis, University of Maryland, 1972
9) F. Ajzenberg-Selove, Nucl. Phys. **A166** (1971) 1
10) E. A. Silverstein, Nucl. Instr. **4** (1969) 53
11) D. F. Measday and C. Richard-Serre, Nucl. Instr. **76** (1969) 45
12) R. Huby and J. R. Mines, Rev. Mod. Phys. **37** (1965) 406
13) W. T. Pinkston and G. R. Satchler, Nucl. Phys. **72** (1965) 641
14) R. H. Philpott, W. T. Pinkston and G. R. Satchler, Nucl. Phys. **A119** (1968) 241
15) R. Huby, Phys. Lett. **33B** (1970) 323
16) D. H. Youngblood *et al.*, Phys. Rev. **C2** (1970) 477
17) W. T. H. van Oers and J. M. Cameron, Phys. Rev. **184** (1969) 1061
18) R. M. Drisko, University of Pittsburgh, unpublished
19) F. G. Perey, Phys. Rev. **131** (1963) 745
20) L. Rosen, J. G. Beery and A. S. Goldhaber, Ann. of Phys. **34** (1965) 96
21) B. Buck, Phys. Rev. **130** (1963) 712
22) E. Newman *et al.*, Nucl. Phys. **A100** (1967) 225
23) F. Hinterberger *et al.*, Nucl. Phys. **A111** (1968) 265
24) H. Doubre *et al.*, Phys. Lett. **29B** (1969) 355
25) G. R. Satchler, Phys. Rev. **C4** (1971) 1485
26) W. P. Beres and W. M. MacDonald, Nucl. Phys. **91** (1967) 529
27) J. F. Sharpey-Schafer, Phys. Lett. **26B** (1968) 652
28) R. P. Singhal, J. R. Moreira and H. S. Caplan, Phys. Rev. Lett. **24** (1970) 73
29) H. A. Bentz, Z. Naturf. **24a** (1969) 858
30) G. W. Greenlees, W. Makofske and G. J. Pyle, Phys. Rev. **C1** (1970) 1145
31) B. A. Watson *et al.*, Phys. Rev. **182** (1969) 977
32) G. M. Lerner, Ph.D. thesis, University of Maryland, 1972
33) J. K. Dickens *et al.*, Phys. Lett. **15** (1965) 337
34) F. G. Perey and D. S. Saxon, Phys. Lett. **10** (1964) 107
35) T. Tamura, W. R. Coker and F. Rybicki, Computer Physics Communications **2** (1971) 94
36) R. H. Bassel, R. M. Drisko and G. R. Satchler, ORNL-3240, unpublished
37) J. L. Alty *et al.*, Nucl. Phys. **A97** (1967) 541
38) I. M. Naqib and L. L. Green, Nucl. Phys. **A112** (1968) 76
39) E. G. deForest, Ph.D. thesis, University of Wisconsin, 1967
40) G. J. Oliver *et al.*, Nucl. Phys. **A127** (1969) 567
41) S. T. Thornton, Nucl. Phys. **A137** (1969) 531
42) G. E. Brown and A. M. Green, Nucl. Phys. **75** (1966) 401
43) R. C. Johnson and F. D. Santos, Proc. Int. Conf. on nuclear structure, Tokyo, 1967, p. 283
44) M. D. Cooper, W. Galati and W. F. Hornyak, submitted for publication
45) R. Lipperheide and K. Möhring, Phys. Lett. **39B** (1972) 323
46) S. Young, Ph.D. thesis, University of Maryland, 1973